



A highly-linear, integration-compatible output metric for amplitude-modulated resonant sensors based on weakly-coupled resonators

Jérôme Juillard, Ali Mostafa, Pietro Maris Ferreira, Manon Gouspy, Michael Kraft

► To cite this version:

Jérôme Juillard, Ali Mostafa, Pietro Maris Ferreira, Manon Gouspy, Michael Kraft. A highly-linear, integration-compatible output metric for amplitude-modulated resonant sensors based on weakly-coupled resonators. 2020 IEEE Sensors, Oct 2020, Rotterdam, Netherlands. 10.1109/SENSORS47125.2020.9278642 . hal-02948372

HAL Id: hal-02948372

<https://hal.science/hal-02948372>

Submitted on 26 Aug 2022

HAL is a multi-disciplinary open access archive for the deposit and dissemination of scientific research documents, whether they are published or not. The documents may come from teaching and research institutions in France or abroad, or from public or private research centers.

L'archive ouverte pluridisciplinaire **HAL**, est destinée au dépôt et à la diffusion de documents scientifiques de niveau recherche, publiés ou non, émanant des établissements d'enseignement et de recherche français ou étrangers, des laboratoires publics ou privés.

A highly-linear, integration-compatible output metric for amplitude-modulated resonant sensors based on weakly-coupled resonators

Jérôme Juillard¹, Ali Mostafa¹, Pietro Maris Ferreira¹, Manon Gouspy^{1,2}, Michael Kraft²

¹GEEPS, UMR CNRS 8507, CentraleSupélec, Université Paris-Saclay, Sorbonne Université, Gif-sur-Yvette, France

²ESAT-MICAS, KU Leuven, Leuven, Belgium

jerome.juillard@centralesupelec.fr

Abstract— In this paper, we propose an alternative output metric for amplitude-modulated resonant sensors based on weakly-coupled resonators. The analog-to-digital conversion of this output metric is less demanding than that of the amplitude ratio, because of its boundedness and of its better linearity. In particular, we show that this output metric provides a perfectly linear measurement of the quantity of interest when a specific resonant sensor architecture based on mutually-injection locked oscillators (MILOs) is used. These results are supported by analytical calculations and by experimental data.

Keywords—resonant sensors, weakly-coupled resonators, injection-locked oscillators, MEMS

I. INTRODUCTION

Resonant MEMS sensors [1] are most often implemented as oscillators, whose main elements are one MEMS resonator and feedback electronics. The electronics pick up the motional signals of the mechanical part and sustain its oscillation by delivering an excitation signal to the resonator, to compensate for dissipative losses and drive it to resonance. When the mechanical stiffness or the mass of the mechanical part changes by a fraction ϵ (proportional to the quantity one seeks to measure, e.g. acceleration, pressure, gas concentration, see [2-4] for some examples), the oscillation frequency of the oscillator changes too. This implementation of frequency-modulated (FM) resonant sensors requires a reference oscillator for demodulating ϵ from the MEMS oscillator output. The main advantage of this architecture is that frequency is a “quasi-digital” quantity, that may be precisely estimated by counting signal zero-crossings, even when the signal is heavily-distorted. One of the shortcomings of the approach is that the reference oscillator should have the same sensitivity to environmental variations in order to discriminate them from changes of ϵ .

To overcome this shortcoming, a “natural” evolution from these concepts emerged in recent years: using a pair of identical resonators (up to fabrication non-idealities) either as two disjoint oscillators for differential FM sensing [5], or as a whole, by introducing an amount of “weak” coupling between the resonators [6,7]. Either implementation provides a differential measurement of ϵ , but the coupled approach opened the way for phase-modulated (PM) or amplitude-modulated (AM) resonant sensors. In a way, this evolution mirrors that of mode-matched MEMS gyroscopes – that can be fundamentally described as two identical resonators coupled through the Coriolis force – from AM architectures to PM and FM architectures [8]. Hence, gyroscopes are close

“cousins” to resonant sensors based on weakly-coupled resonators (WCRs).

AM WCR architectures have the same limitations and advantages as AM gyroscope architectures: on the one hand, they are sensitive to distortion and have to face the bottleneck of analog-to-digital conversion but, on the other hand, analog-to-digital converters (ADCs) may arguably be implemented at a lesser cost than precision oscillators required for FM architectures. Furthermore, AM WCRs are not subject to limitations induced by resonator nonlinearity [9], such as the A-f effect [10], which limits the use of conventional FM and PM WCRs (and also of conventional FM resonant sensors). A peculiarity of AM WCRs is that their output metric of choice [6] is the ratio R of the oscillation amplitudes of the two resonators (which oscillate in a synchronous way, at the same oscillation frequency). While R is an intrinsically differential output metric, it is also an intrinsically nonlinear function of ϵ for all WCR architectures that have been proposed to this day. Thus the sensitivity of R to ϵ is not uniform across the sensor dynamic range, and this makes impractical the use of an ADC with uniform quantization levels.

In this paper, we propose an alternative output metric T for AM WCRs with a better linearity across the sensor dynamic range. We also show for the first time that this output metric provides a perfectly linear measurement of the quantity of interest ($T \propto \epsilon$) when a specific WCR architecture based on mutually-injection locked oscillators (MILOs) is used. In section II, this output metric is defined and its properties are established. In section III, we compare this output metric to others with simulated and experimental data. Conclusions are presented in section IV.

II. A NEW OUTPUT METRIC FOR AM WCRS

A. Framework

We consider two nominally-identical coupled resonators with quality factor $Q \gg 1$, and natural frequency f_0 , as represented in Fig 1-a. The physical quantity of interest induces a relative stiffness change ϵ in one resonator, and $-\epsilon$ in the other. The resonators oscillate synchronously with frequency $f \approx f_0$ over a certain range $\pm\epsilon_{lock}$ of values of ϵ , thanks to some electronics (which may also provide the coupling, in the case of MILO architectures). The oscillation amplitudes of the resonators are $X_1(\epsilon)$ and $X_2(\epsilon)$. In the nominal case ($\epsilon = 0$), we have $X_1(0) = X_2(0)$ so that $R(0) = 1$.

B. Definition and fundamental properties

The proposed output metric is defined as

$$T(\epsilon) = 2 \frac{X_1(\epsilon) - X_2(\epsilon)}{X_1(\epsilon) + X_2(\epsilon)} = 2 \frac{R(\epsilon) - 1}{R(\epsilon) + 1}$$

This modified amplitude ratio, which may be called “bilinear” with respect to the bilinear transform, was initially proposed in [11], in a different context. By construction, it has the same sensitivity as $R(\epsilon)$ near $\epsilon = 0$, but several other properties make it more interesting. First of all, $T(\epsilon)$ is intrinsically bounded (between -2 and 2), whereas $R(\epsilon)$ is not. Moreover, for the most common AM MILO architectures, $T(\epsilon)$ is odd, whereas $R(\epsilon)$ is not. Thus, the bilinear amplitude ratio is “better-behaved” than the classical amplitude ratio. Furthermore, from a practical perspective, it is possible to digitize $T(\epsilon)$ from the amplitudes $X_1(\epsilon)$ and $X_2(\epsilon)$ without having to implement electronic blocks for the addition and subtraction of these quantities, or for the division. To this end, [11] proposes a continuous architecture of a “ratiometric” $\Delta\Sigma$ -ADC, a discrete-time version of which was proposed in our own work [12], as shown in Fig. 2.

Finally, the bilinear amplitude ratio has a remarkable property for specific MILO architectures, as explained in the next section.

C. Properties of the bilinear amplitude ratio for MILOs

In a MILO resonant sensor, coupling is enforced through the resonators’ feedback electronics. The electronics serve not only to sustain resonator motion, but also to “mix” their signals and enforce their synchronization over a certain locking range. As described in [7], several different architectures, with different properties in terms of sensitivity, resolution and range, and with different output metrics, can be derived from this generic principle. In particular, as shown in [9], some MILO architectures can be used both as PM and AM resonant sensors, depending on the amount of phase-shift θ in the branches of the mixer (Fig. 1-b).

Let us first focus on the properties of the architecture studied shown in Fig 1-b, when $\theta = 45^\circ$. In this case, when $\epsilon = 0$, both resonators are driven at resonance and oscillate in quadrature, at f_0 . When ϵ changes, the oscillation frequency does not deviate significantly from f_0 , but the phase difference between the resonators changes and their oscillation amplitudes change also. It is straightforward to show that we have precisely

$$R(\epsilon) = \frac{1 + Q\epsilon}{1 - Q\epsilon}$$

$$T(\epsilon) = 2Q\epsilon$$

Thus, while the amplitude ratio R is a nonlinear functions of ϵ , the bilinear amplitude ratio T is perfectly linear with ϵ across the locking range. In the case $\theta = 135^\circ$, the same expressions hold, and $T(\epsilon)$ is also perfectly linear.

In the case $\theta = 90^\circ$, which may also be used for AM resonant sensing [9], we find

$$R(\epsilon) = \frac{\sqrt{1 + (Q\epsilon)^2} + Q\epsilon}{\sqrt{1 + (Q\epsilon)^2} - Q\epsilon}$$

$$T(\epsilon) = 2Q\epsilon/\sqrt{1 + (Q\epsilon)^2}$$

Even in this case, $T(\epsilon)$ has much better linearity than $R(\epsilon)$, as illustrated in the next section.

III. RESULTS

A. Simulation

In Fig. 3, we plot $R(\epsilon)$ and $T(\epsilon)$ for two MILO architectures, one with $\theta = 45^\circ$, and one with $\theta = 90^\circ$. This illustrates that, even in the case $\theta = 90^\circ$ when $T(\epsilon)$ is not perfectly linear, it is better-behaved than $R(\epsilon)$ over the locking range ($\epsilon_{lock} = Q/\sqrt{2}$ for both architectures). The RMS linearity error with respect to the straight line $2Q\epsilon$ (tangent at origin in all the cases) is reported in table I.

B. Experimental results

The same setup as in [13] is used for our experiments: two resonators with capacitive actuation and detection are coupled through a MILO architecture, whose characteristic phase-shift is $\theta = 45^\circ$. A relative stiffness mismatch can be induced between the two resonators through electrostatic softening, by varying the bias voltage of one of the resonators. A good estimation of ϵ can be inferred from the model developed in [13], from the characterization of the different elements of the oscillator, and from measurements of the duty cycles and oscillation amplitudes of the motional signals. In Fig. 4, we plot $R(\epsilon)$ and $T(\epsilon)$, as obtained from the estimated from the RMS amplitudes of the motional signals. In spite of strong detection nonlinearity (the mechanical oscillation amplitude is about 40% of the gap), in spite of many other non-idealities (electromechanical coefficient mismatch, quality factor mismatch, nonlinear damping, comparator hysteresis, actuation nonlinearity, among others), the same tendencies as in the ideal case can be found. Over the observable locking range (about one half of the ideal locking range can be observed, because of non-idealities), we find the error between the measured data and the best fit straight line to be 4 times as small for $T(\epsilon)$ than for $R(\epsilon)$. Note that this error is not only due to “intrinsic” output metric nonlinearity, but also to measurement noise.

IV. CONCLUSION

In this paper, we have highlighted some remarkable properties of the bilinear amplitude ratio T over the classical amplitude ratio R , when used in conjunction with MILO-based resonant sensors. Our calculations in an ideal case showed that T could be perfectly linear with resonator stiffness mismatch for specific MILO architectures, and provided a general improvement in terms of linearity outside of these specific cases. Experimental measurements indicated that this improvement was quite robust to several non-idealities, such as those resulting from fabrication dispersions. Similar results can be observed for other WCR architectures, such as those based on mode-localization. Finally, as shown in [11-12], the bilinear amplitude ratio is amenable to integration and high-resolution analog-to-digital conversion.

TABLE I. CALCULATED LINEARITY ERROR

	$\theta = 45^\circ$		$\theta = 90^\circ$	
	$R(\epsilon)$	$T(\epsilon)$	$R(\epsilon)$	$T(\epsilon)$
RMSE	0.85	0	0.46	0.10

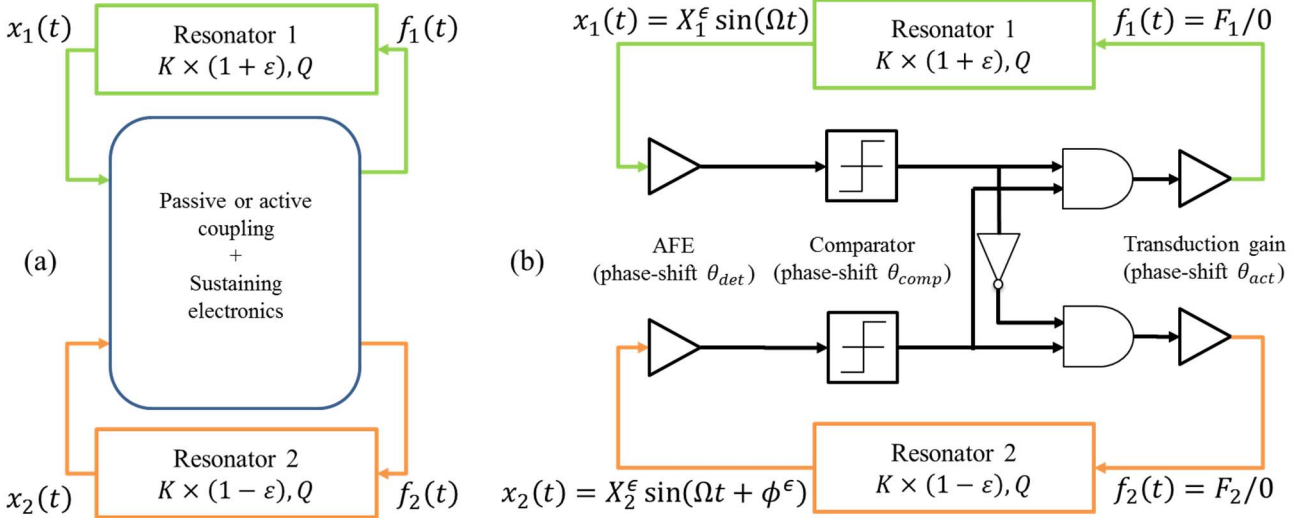


Fig. 1. (a) System-level representation of a resonant sensor based on WCRs. (b) System-level representation of a MILO using a digital mixer. Parameter θ is the sum of the phase-shifts in the elements of the loop.

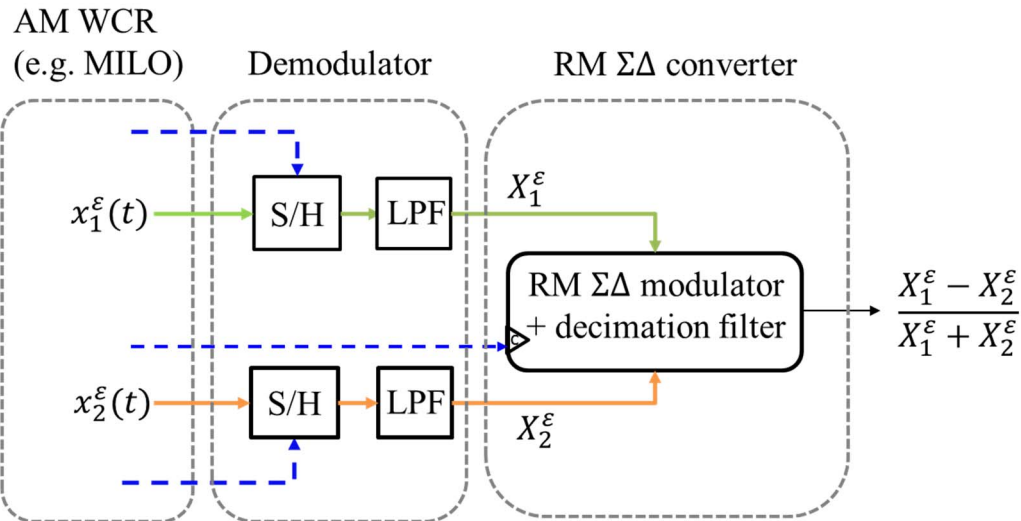


Fig. 2. System-level representation of a ratiometric AM WCR with digital output consisting of an AM WCR, an analog amplitude demodulation block (sample-hold + lowpass filter) and a ratiometric $\Sigma\Delta$ converter [11-12]. The sampling frequency can be generated in the WCR (e.g. comparator outputs).

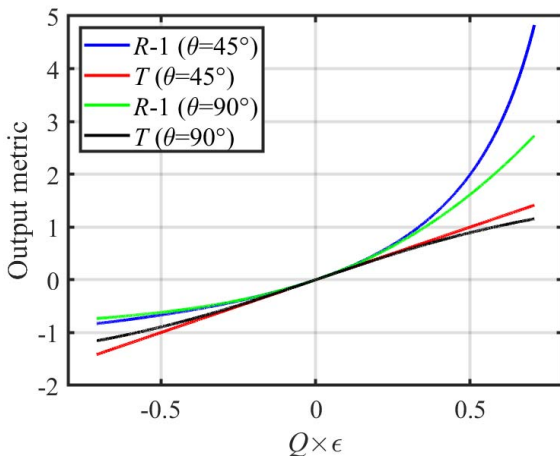


Fig. 3. Comparison of $R(\varepsilon)$ and $T(\varepsilon)$ for two MILO architectures ($\theta = 45^\circ$ and $\theta = 90^\circ$).

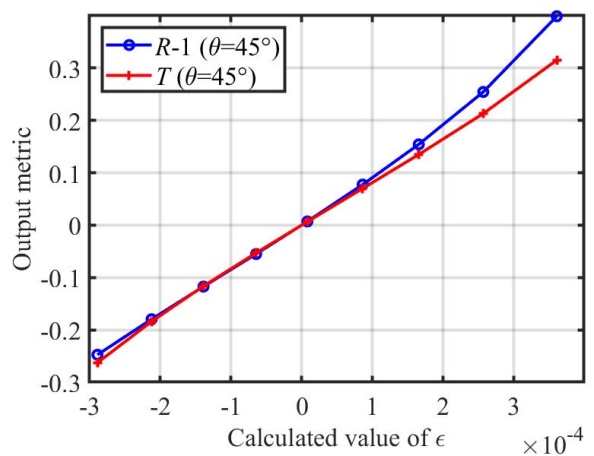


Fig. 4. Comparison of $R(\varepsilon)$ and $T(\varepsilon)$ for the MILO architecture of [13] ($\theta \approx 45^\circ$, $Q \approx 15000$, $f_0 \approx 68\text{kHz}$, $V_{bias} \approx 40V$, $V_{drv} \approx 450mV$).

REFERENCES

- [1] G. Stemme, "Resonant silicon sensors", , Journal of Micromechanics and Microengineering, vol. 1, 1991
- [2] A. Caspani et al., "Compact biaxial micromachined resonant accelerometer", Journal of Micromechanics and Microengineering, vol. 23, 2013
- [3] K. Hsieh, J. Chiu, M. S. Lu, "Development of CMOS micromachined capacitive squeeze-film pressure sensors", IEEE Sensors Journal, 2020
- [4] K .L. Ekinci, X. M. H. Huang, M. L. Roukes, "Ultrasensitive nanoelectromechanical mass detection", Applied Physics Letters, vol. 84 (22), pp. 4469-4471, 2004
- [5] C. Cobianu, B. Serban, "All-differential resonant nanosensor apparatus and method", US Patent 0113856 A1, 2011
- [6] C Zhao et al., "A review on coupled MEMS resonators for sensing applications utilizing mode localization", Sensors and Actuators A, vol. 249, pp. 93-111, 2016
- [7] J. Juillard, P. Prache? N. Barniol, "Analysis of Mutually Injection-Locked Oscillators for Differential Resonant Sensing", IEEE Transactions on Circuits and Systems I, vol. 63 (7), pp. 1055-1066, 2016
- [8] M. Kline, "Frequency-modulated gyroscopes", Ph.D. Thesis, U. of California, Berkeley, 2013
- [9] J. Juillard, A. Mostafa, P. M. Ferreira, "Nonlinear operation of resonant sensors based on weakly coupled resonators: theory and modeling", IEEE Transactions on Ultrasonics, Ferroelectrics and Frequency Control, vol. 66, pp. 1950-1961, 2019
- [10] R. Lifschitz, M. C. Cross, "Nonlinear dynamics of nanomechanical and micromechanical resonators," in Review of Nonlinear Dynamics and Complexity Hoboken, NJ, USA: Wiley, 2008.
- [11] A. Fekri et al., "An eddy-current displacement-to-digital converter based on a ratio-metric delta-sigma ADC", 40th European Solid State Circuits Conference (ESSCIRC), 2014, pp. 403–406
- [12] A. Mostafa, J. Juillard, J. R. Raposo, P. M. Ferreira, "An adaptative ratio-metric analog-to-digital interface for weakly-coupled resonant sensors based on mutually injection-locked oscillators", Symposium on Design, Test, Integration and Packaging of MEMS/MOEMS (DTIP), 2019, pp. 1-4
- [13] J. Juillard, A. Mostafa, P. M. Ferreira, "Nonlinear operation of resonant sensors based on weakly coupled resonators: experimental investigation of an actively-coupled architecture", Sensors and Actuators A, vol. 297, 111504, 2019